Review

Molecular Dynamics Simulation Studies of Properties, Preparation, and Performance of Silicon Carbide Materials: A Review

Zefan Yan, Rongzheng Liu, Bing Liu, Youlin Shao and Malin Liu *

Institute of Nuclear and New Energy Technology, Tsinghua University, Beijing 100084, China
* Correspondence: liumalin@tsinghua.edu.cn

Abstract: Silicon carbide (SiC) materials are widely applied in the field of nuclear materials and semiconductor materials due to their excellent radiation resistance, thermal conductivity, oxidation resistance, and mechanical strength. The molecular dynamics (MD) simulation is an important method to study the properties, preparation, and performance of SiC materials. It has significant advantages at the atomic scale. The common potential functions for MD simulations of silicon carbide materials were summarized firstly based on extensive literatures. The key parameters, complexity, and application scope were compared and analyzed. Then, the MD simulation of SiC properties, preparation, and performance was comprehensively overviewed. The current studies of MD simulation methods and applications of SiC materials were systematically summarized. It was found that the Tersoff potential was the most widely applied potential function for the MD simulation of SiC materials. The construction of more accurate potential functions for special application fields was an important development trend of potential functions. In the MD simulation of SiC properties, the thermal properties and mechanical properties, including thermal conductivity, hardness, elastic modulus, etc., were mainly studied. The correlation between MD simulations of microscopic processes and the properties of macroscopic materials, as well as the methods for obtaining different property parameters, were summarized. In the MD simulation of SiC preparation, ion implantation, polishing, sputtering, deposition, crystal growth, amorphization, etc., were mainly studied. The chemical vapor deposition (CVD) and sintering methods commonly applied in the preparation of SiC nuclear materials were reported rarely and needed to be further studied. In the MD simulation of SiC performance, most of the present studies were related to SiC applications in the nuclear energy research. The irradiation damage simulation in the field of nuclear materials was studied most widely. It can be found that SiC materials in the field of nuclear materials study were a very important topic. Finally, the future perspective of MD simulation studies of SiC materials were given, and development suggestions were summarized. This paper is helpful for understanding and mastering the general method of computation material science aimed at the multi-level analysis. It also has a good reference value in the field of SiC material study and MD method study.

Keywords: silicon carbide; molecular dynamics simulation; property; preparation; performance

Citation: Yan, Z.; Liu, R.; Liu, B.; Shao, Y.; Liu, M. Molecular Dynamics Simulation Studies of Properties, Preparation, and Performance of Silicon Carbide Materials: A Review. *Energies* **2023**, *16*, 1176. https://doi.org/10.3390/en16031176

Academic Editor: Attilio Converti

Received: 9 December 2022
Revised: 18 January 2023
Accepted: 19 January 2023
Published: 20 January 2023

Copyright: © 2023 by the authors. Licensee MDPI, Basel, Switzerland. This article is an open access article distributed under the terms and conditions of the Creative Commons Attribution (CC BY) license (https://creativecommons.org/licenses/by/4.0/).

1. Introduction

Silicon carbide (SiC) materials have attracted much attention in the fields of new nuclear materials [1–3] and semiconductor materials [4], due to their excellent irradiation resistance, thermal conductivity, oxidation resistance, and mechanical strength. There are many experimental and simulation studies of SiC materials that have been reported on the properties, preparation methods, and performance, especially the irradiation performance. In recent years, there are many new achievements in the simulation of properties, preparation, and performance of SiC materials based on molecular dynamics (MD) simulation with the development of computational materials science, simulation resources, and simulation

methods. The development of SiC materials in the material design, application scenarios, and evaluation of new nuclear energy systems and semiconductor electronic systems are contributed greatly by these achievements.

The properties of SiC materials depend on their strong covalent bonds and stable crystal structures [5]. There are two main crystal structures of SiC, called β-SiC (low-temperature stable cubic crystal system, also known as 3C-SiC) and α-SiC (high-temperature stable hexagonal crystal system). They consist of covalently bonded tetrahedral basic units. The perfect symmetry and strong anisotropy of the crystal structure of SiC materials are determined by their structural features. It results in fewer atomic slip surfaces, less deformations, and high strength at high temperatures [6]. There are some kinds of α-SiC variants, including 4H, 6H, 15R, etc., due to the different stacking patterns of the structural unit layers [7]. Although the densities of SiC polymorphs are close, there are differences in the stability at different temperatures. β-SiC is stable below 2100 °C and starts to transform into α-SiC above 2100 °C [5]. Therefore, SiC synthesized below 2000 °C is mainly β-SiC, while when synthesized above 2200 °C it is mainly α-SiC (predominantly 6H). In addition to typical SiC crystal materials (3C, 4H, 6H, etc.), SiC nanotubes, SiC nanocages, SiC nanosheets, amorphous SiC, etc., are also involved in MD simulation studies.

The MD method [8] is an efficient and convenient analytical tool to study the SiC preparation, properties, and performance. MD is a method of applying the concept of classical mechanics to atomic and molecular systems. According to classical mechanics, the total energy of the system is calculated from the position of the atoms, the bonding mode, the potential function, and the velocity of the atoms. Then, the potential energy gradient of the atom in the force field is calculated from the total energy. The forces acting on an atom are equal to the negative value of the potential gradient at the position of the atom. The behavior of the atom's motion can be calculated according to Newton's second law after the forces on each atom in the force field have been calculated. The trajectories of the atoms in phase space (space of atomic positions and momentum coordinates) will be obtained after the required number of loop iterations. Therefore, the macroscopic property parameters of the material can be calculated using appropriate relationships between microscopic and macroscopic parameters.

In this paper, the MD potential functions of SiC materials were compared at first. The advances in MD simulation of the properties (thermal properties, mechanical properties, etc.), preparation (ion implantation, polishing, sputtering, etc.), and performance (irradiation damage, shock damage, etc.) of SiC materials were systematically reviewed. The comparative analysis and future study prospects were given accordingly. The purpose is to sort out the relevant advances in MD simulation studies of SiC materials as comprehensively as possible to provide references and contribute to the in-depth study of the preparation and application of SiC materials.

2. Comparative Analysis of Potential Functions for MD Simulation of Silicon Carbide

The choice of potential function is the most important in MD simulation. A variety of potential functions have been used in the MD simulation of SiC materials. A comprehensive summary of the potential functions for MD simulations of SiC materials was provided in this section. The application scenarios and scope are analyzed, as shown in Table 1. The specific form and the variable meaning of each potential function are summarized in detail, as follows.

Table 1. The common potential functions for MD simulations of silicon carbide materials.

Potential Function	Key Parameter	Complexity	Application
Tersoff [9,10]	Cutoff function, Two-body potential, Three-body potential	Simple	Thermal properties, Mechanical properties, Electrical properties, Ion implantation, Polishing, Sputtering, Crystal growth, Amorphization, Sintering, Irradiation damage, Fatigue damage, Shock damage
Tersoff/Ziegler-Biersack-Littmark (ZBL) [11,12]	Cutoff function, Two-body potential, Three-body potential, Connection function, ZBL potential	General	Ion implantation, Irradiation damage
Vashishta [13,14]	Two-body potential, Three-body potential	Simple	Mechanical properties, Electrical properties, Polishing, Deposition, Shock damage
Environment-Dependent Interatomic Potential (EDIP) [15,16]	Two-body potential, Three-body potential	General	Mechanical properties
Modified Embedded-Atom Method (MEAM) [17–19]	Pair potential interaction, Embedding energy	Complex	Thermal properties, Crystal growth, Irradiation damage
Gao-Weber [20]	Cutoff function, Two-body potential, Three-body potential	Simple	Irradiation damage
Gao-Weber/ZBL [21]	Cutoff function, Two-body potential, Three-body potential, Connection function, ZBL potential	General	Crystal growth, Irradiation damage

2.1. Tersoff Potential

The Tersoff potential is based on the concept of the bond order in quantum mechanics and the relationship between the bond order and the surrounding environment [9,10]. The basic form of the Tersoff potential is given as follows

$$E = \frac{1}{2}\sum_{i}\sum_{j\neq i} V^{Tersoff}(r_{ij}) = \frac{1}{2}\sum_{i}\sum_{j\neq i}\{f_C(r_{ij})[f_R(r_{ij}) + b_{ij}f_A(r_{ij})]\}, \quad (1)$$

$$f_R(r_{ij}) = A\exp(-\lambda_1 r_{ij}), \quad (2)$$

$$f_A(r_{ij}) = -B\exp(-\lambda_2 r_{ij}). \quad (3)$$

where E is the total energy of the system. It is the sum of all interatomic bond energies calculated by the Tersoff potential $V^{Tersoff}$. f_R is a two-body potential, representing the repulsion and including the orthogonalization energy when the atomic wave functions overlap. f_A is the bonding-related attraction. b_{ij} is the bond order connecting atoms i and j, representing the local bonding and determining the dependence of the potential on the bond angle. The product of f_A and b_{ij} is the three-body potential. f_C is a cutoff function used to limit the range of the potential, so the interaction between two atoms tends smoothly to zero at a distance. r_{ij} is the distance between atoms i and j. r_{ik} is the distance between atom i and atom k. A, B, λ_1, and λ_2 are the relevant constants.

2.2. Tersoff/ZBL Potential

The Tersoff/ZBL potential is the Tersoff potential with a short-range, pairwise modification based on the ZBL potential [11,12]. The basic form of the Tersoff/ZBL potential is listed as follows

$$E = \frac{1}{2}\sum_{i}\sum_{j\neq i}\{[1 - f_F(r_{ij})]V^{ZBL}(r_{ij}) + f_F(r_{ij})V^{Tersoff}(r_{ij})\}, \quad (4)$$

$$V^{ZBL}(r_{ij}) = \frac{Z_i Z_j}{4\pi\varepsilon_0 r_{ij}} \times \psi(r_{ij}/\alpha) \quad (5)$$

where V^{ZBL} is the ZBL potential, and f_F is the fermi-like function used to smoothly connect the ZBL potential and the Tersoff potential. In the ZBL potential, the first term represents the repulsive effect of the Coulomb force. Z_i and Z_j are the charges of atoms i and j. ε_0 is the vacuum dielectric constant. The second term is the universal screening function Ψ for most atomic systems with a distance of less than 1 Å. α is the Bohr radius corrected by the atomic charge.

2.3. Vashishta Potential

The Vashishta potential considers Coulomb force, charge-dipole interaction, van der Waals force, steric repulsion, and three-body interaction [13,14]. The basic form of the Vashishta potential is listed as follows

$$E = \sum_i \sum_{j>i} V_2^{Vash}(r_{ij}) + \sum_i \sum_{j\neq i} \sum_{k>j,k\neq i} V_3^{Vash}(r_{ij}, r_{ik}), \quad (6)$$

$$V_2^{Vash}(r_{ij}) = \frac{H}{{r_{ij}}^{\eta}} + \frac{Z_i Z_j}{r_{ij}} \exp(-r_{ij}/\tau_1) - \frac{D}{{r_{ij}}^4} \exp(-r_{ij}/\tau_4) - \frac{W}{{r_{ij}}^6}, \quad (7)$$

$$V_3^{Vash}(r_{ij}, r_{ik}) = R_3^{Vash}(r_{ij}, r_{ik}) P_3^{Vash}\left(\theta_{jik}\right). \quad (8)$$

where V_2^{Vash} is the two-body potential part and V_3^{Vash} is the three-body potential part. In the two-body potential, the first term is the steric repulsion term, representing the steric size effect of the ions. The second term is the Coulomb term, representing the charge transfer effect leading to the Coulomb interaction. The third term is the charge-dipole term, representing the charge-dipole interaction due to the electronic polarizability of the ions. The fourth term is the van der Waals term, representing the induced van der Waals interaction. H, η, D, τ_1, τ_4, and W are the relevant constants. In the three-body potential, the first term, R_3^{Vash}, is a radial function, representing the spatial dependence. The second term, P_3^{Vash}, is an angular function, representing the angular dependence. θ_{jik} is the bond angle formed by the ij bond and ik bond.

2.4. EDIP

The EDIP is a potential, describing the dependence of chemical bonds on local coordination numbers [15,16]. The basic form of the EDIP is listed as follows

$$E = \sum_{j\neq i} V_2^{EDIP}(r_{ij}, X_i) + \sum_{j\neq i} \sum_{k\neq i,k>j} V_3^{EDIP}(r_{ij}, r_{ik}, X_i), \quad (9)$$

$$V_2^{EDIP}(r_{ij}, X_i) = M[\left(\frac{N}{r_{ij}}\right)^{\mu} - e^{-\beta X_i^2}] R_2^{EDIP}(r_{ij}), \quad (10)$$

$$V_3^{EDIP}(r_{ij}, r_{ik}, X_i) = R_3^{EDIP}(r_{ij}, r_{ik}) P_3^{EDIP}(\theta_{jik}, X_i), \quad (11)$$

$$X_i = \sum_{m\neq i} f_C^{EDIP}(r_{im}). \quad (12)$$

where V_2^{EDIP} is the two-body potential part, and V_3^{EDIP} is the three-body potential part. Both parts depend on the effective coordination number X_i of atom i. X_i is calculated by the cutoff function f_C^{EDIP}. The contribution of atom i to the coordination, according to the distance r_{im} from atom i to its neighbor atom m, is calculated by f_C^{EDIP}. The two-body potential contains repulsive and attractive interactions. R_2^{EDIP} is a radial function. M, N, μ, and β are the relevant constants. The three-body potential of EDIP is similar to the Vashishta potential. It is the product of the spatial-dependent term R_3^{EDIP} and the angular-dependent term P_3^{EDIP}. P_3^{EDIP} strongly depends on the local coordination by controlling the equilibrium of the bond angle and interaction strength.

2.5. MEAM Potential

The embedded-atom method (EAM) potential is inspired by the density functional theory and adds an energy functional of the local electron density on the basis of the pair potential interaction. The MEAM potential improves the electron density as a function of angle dependence, based on the EAM potential [17–19]. The basic form of the MEAM potential is listed as follows

$$E = \sum_i \left\{ F(\overline{\rho}_i) + \frac{1}{2}\sum_{i \neq j} \varphi_{(rij)} \right\}, \quad (13)$$

$$\overline{\rho}_i = \sum_{j \neq i} \rho_j(r_{ij}). \quad (14)$$

where φ is the pair potential interaction between atoms. F is the embedding energy of atom i embedded in an electron cloud. It is the energy functional of atoms embedded in a uniform electron gas with density $\overline{\rho_i}$. $\overline{\rho_i}$ is an estimate of the local electron density at the position of atom i. This can be approximated as the sum of the electron density ρ_j contributed by the neighbor atoms of atom i.

2.6. Gao-Weber Potential

The Gao-Weber potential is similar to the Tersoff potential, but includes additional parameters for explaining the atomic chemical environment [20]. The basic form of the Gao-Weber potential is listed as follows

$$E = \sum_i \sum_{j(>i)} V^{GW}(r_{ij}) = \sum_i \sum_{j(>i)} \{f_C^{GW}(r_{ij})[f_R^{GW}(r_{ij}) + \overline{B}_{ij} f_A^{GW}(r_{ij})]\}, \quad (15)$$

$$f_A^{GW}(r_{ij}) = -[D_c S/(S-1)] \times \exp[-\omega\sqrt{2/S}(r_{ij} - R_c)], \quad (16)$$

$$f_R^{GW}(r_{ij}) = [D_c S/(S-1)] \times \exp\left[-\omega\sqrt{2S}(r_{ij} - R_c)\right]. \quad (17)$$

where V^{GW} is the Gao-Weber potential. f_R^{GW} is a two-body potential, representing repulsion. f_A^{GW} represents attraction. $\overline{B}_{ij}$ is the bond order connecting atoms i and j. The product of f_A^{GW} and $\overline{B}_{ij}$ is the three-body potential. f_C^{GW} is the cutoff function. D_c, R_c, ω, and S are the relevant constants.

2.7. Gao-Weber/ZBL Potential

The Gao-Weber/ZBL potential is combined by the Gao-Weber potential and the ZBL potential; thus its disadvantage in describing the short-range interaction is improved. The combination is similar to the Tersoff/ZBL potential, with more details given, as shown in [21].

2.8. Comparative Analysis

SiC is a typical covalent bonding material, and its common potential functions are all closely related to the bond angle. The bonding characteristics of covalent materials are well described by these potential functions, such as strong directionality, dynamic variability, and complexity, thus the nature and structure of SiC materials can be described accurately. The Si-C interatomic interaction curves of the SiC common potential functions were summarized, as shown in Figure 1. In the long-range (>3 Å) and medium-range (>1 Å and <3 Å), other potential functions have little difference, except the MEAM potential and Vashishta potential. In the short-range (<1 Å), EDIP has the lowest energy. In the extremely short range (<0.2 Å), the Vashishta potential has the fastest energy growth.

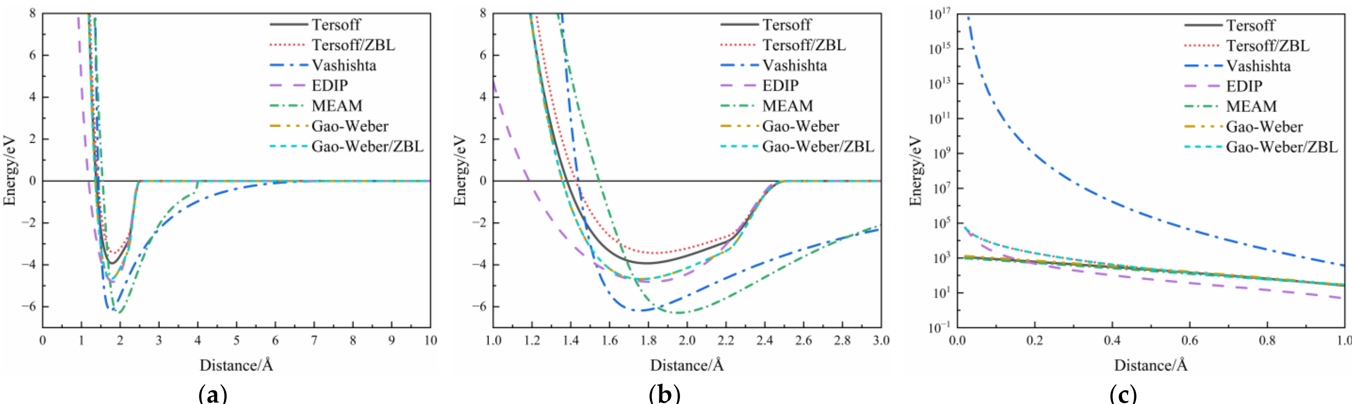

Figure 1. The Si-C interatomic interaction curves of the SiC potential functions: (**a**) Overview; (**b**) Medium-range; (**c**) Short-range [10,11,14,16,19–21].

The Tersoff potential is a simple bond order potential, which provides a sufficiently accurate description of the interaction between covalently bonded atoms and achieves an excellent balance between computational accuracy and speed. A series of Tersoff potential versions have been developed for SiC materials [10,22–24]. Therefore, the Tersoff potential was widely applied in the properties, preparation, and performance of SiC materials and showed excellent simulation results. It is the most popular potential in the MD simulation of SiC materials.

The Tersoff/ZBL potential adds a ZBL potential that specifically describes the short-range interaction to the Tersoff potential, allowing for a more accurate description of the equilibrium properties and short-range atomic collisions of SiC. In the MD study of SiC, the Tersoff/ZBL potential was first successfully applied to the simulation of irradiation damage. It was also later applied to the simulation of ion implantation.

The Vashishta potential considers the ionic bond characteristics based on the covalent bond characteristics of SiC, so the Coulomb, steric repulsion, and other interactions are included in its two-body potential part. Its three-body potential part is inspired by the Stillinger-Weber potential [25], considering the spatial and angular dependence. The bending and stretching of covalent and ionic bonds of SiC can be described accurately by the Vashishta potential; thus the structural energy, structural transformation, and stacking fault energy of SiC materials can be accurately computed. In the MD study of SiC, the Vashishta potential was first applied to simulate crystallization and amorphous behavior. It was also later applied to the simulations of mechanical properties, electrical properties, polishing, deposition, shock damage, etc.

The EDIP is formally inspired by the Stillinger-Weber potential and introduces the atomic coordination numbers into the potential function. The phenomenon that the attraction interaction decreases, and the bond length increases with the increase in the coordination numbers, can be described accurately by its two-body potential part. Its three-body potential part is similar to the Vashishta potential. However, the transition from covalent to metallic bonds as the coordination numbers increase can be accurately described. The EDIP potential has an advantage over the Tersoff potential in describing the local bonding of bulk defects and disordered phases. It is also faster in the calculation. In the MD study of SiC, the EDIP was mainly applied to the simulation of mechanical properties.

The MEAM potential retains the advantages of the EAM potential, as the energy of distributed electrons and the change of asymmetric local bonding can be described accurately. The disadvantage that the EAM potential does not reflect the directionality and angle in the electron density to accurately describe covalent bonding materials, such as SiC, is also solved. In the MD study of SiC, the MEAM potential is accurate in describing defects, and was successfully applied to the simulation of irradiation damage, thermal properties, crystal growth, etc.

The Gao-Weber potential is similar to the Tersoff potential in form. However, various equilibrium properties and stable defect configurations of SiC are considered. Therefore, the properties of SiC defects can be computed more accurately. In the MD study of SiC, the Gao-Weber potential was mainly applied to the simulation of irradiation damage. A more realistic irradiation simulation can be provided by the Gao-Weber/ZBL potential, due to the inclusion of the ZBL potential. In the MD study of SiC, the Gao-Weber/ZBL potential was first successfully applied to the simulation of irradiation damage. It was later also applied to the simulation of crystal growth.

3. MD Simulation Studies of Silicon Carbide Materials

The MD simulation of SiC materials is extensively studied. From the four elements of material study, there are many MD simulation studies on the properties, preparation, and performance of SiC based on the composition. The studies reported in recent years are summarized, as shown in Table 2.

Table 2. The overview of MD simulation studies on silicon carbide materials.

	Simulation Field	Study Content	Type of SiC	Simulation Characteristic
Properties	Thermology [26–32]	Thermal conductivity	3C-SiC, SiC nanotubes, SiC/SiC composites, SiC crystal/amorphous layers	Calculation of thermal conductivity by the equilibrium molecular dynamics (EMD), the nonequilibrium molecular dynamics (NEMD), and the reverse nonequilibrium molecular dynamics (RNEMD).
	Mechanics [33–41]	Hardness, Elastic modulus, Strength	3C-SiC, 2H-SiC, 4H-SiC, 6H-SiC, SiC nanosheets	Calculation of hardness, elastic modulus, and strength by uniaxial tension/compression, nanoindentation.
	Electricity [42,43]	Dielectric constant	3C-SiC	Calculation of dielectric constant of SiC by the linear response theory.
Preparation	Ion implantation [38,39,44–49]	Si ion implantation H ion implantation Metal ion implantation	3C-SiC, 4H-SiC, 6H-SiC	Effects of ion implantation on defect evolution, mechanical properties, and machinability.
	Polishing [50–63]	Abrasive polishing Tool polishing Assisted polishing	3C-SiC, 4H-SiC, 6H-SiC	Removal and deformation mechanism of surface in polishing.
	Sputtering [64–69]	Inert substance sputtering Reactive substance sputtering	3C-SiC, 4H-SiC	Sputtering mechanism, sputtering yield, and sputtering products on surface.
	Deposition [70–73]	Physical deposition	4H-SiC, Amorphous SiC	Effects of atomic incident energy, substrate morphology, and substrate temperature on the quality of deposited films.
	Crystal growth [19,21,74,75]	Crystal growth at solid/liquid interface	3C-SiC, 4H-SiC, 6H-SiC	Crystallization behavior and mechanism.
	Amorphization [76–79]	Heating amorphization Cooling amorphization	SiC nanosheets, SiC nanoribbons, SiC nanobelts	Structural evolution and mechanism of amorphization.
	Sintering [80]	Nanoparticle sintering	SiC nanoparticles	Sintering process and mechanism of nanoparticles.
	New-type SiC materials [81]	Preparation of nanocage	SiC nanocages	Properties and preparation feasibility of nanocage structure.

Table 2. *Cont.*

Simulation Field		Study Content	Type of SiC	Simulation Characteristic
Performance	Irradiation damage [28,29,31,36,82–92]	Effect of irradiation on properties	3C-SiC, 4H-SiC, 6H-SiC, SiC/SiC composites	Effects of defects induced by irradiation damage on thermal and mechanical properties.
		Mechanism of irradiation damage		Formation process and mechanism of irradiation defects, recovery mechanism of irradiation defects, and formation mechanism of irradiation swelling.
	Fatigue damage [37,93]	Crack	SiC nanosheets	Evolution of cracks under external force and its effect on mechanical properties.
	Shock damage [94–96]	Shock response	3C-SiC, 4H-SiC, 6H-SiC	Effects of shock velocity on shock response.

3.1. MD Simulation Studies of Silicon Carbide Properties

3.1.1. MD Simulation Studies of SiC Thermal Properties

The MD simulation study of SiC thermal properties mainly focuses on the calculation of thermal conductivity. The typical thermal conductivity calculation model of SiC was given, as shown in Figure 2. There are three kinds of methods to calculate the thermal conductivity, called the EMD (the equilibrium molecular dynamics), the NEMD (the nonequilibrium molecular dynamics), and the RNEMD (the reverse nonequilibrium molecular dynamics).

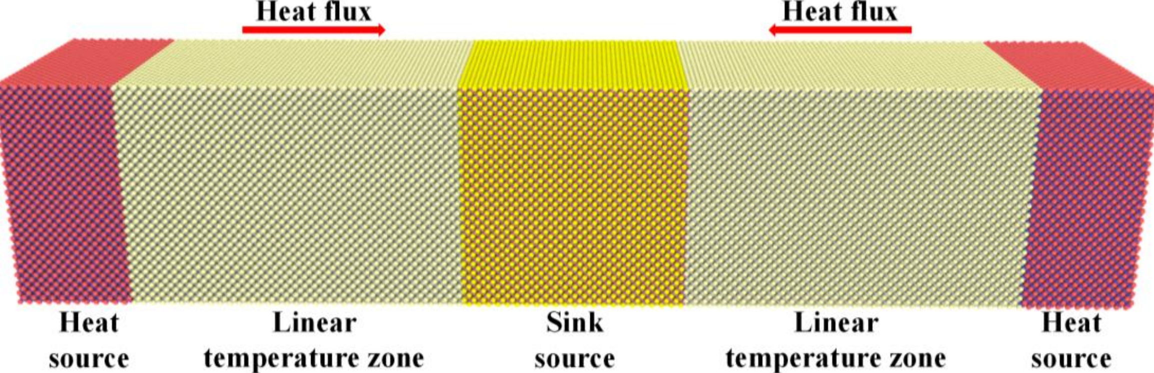

Figure 2. The typical thermal conductivity calculation model of SiC [28].

The EMD method is based on the Green-Kubo theory, and the NEMD method and the RNEMD method are based on the Fourier theory. The difference between the NEMD method and the RNEMD method is the way the temperature gradient is generated. A constant temperature difference at both ends of the material are applied directly by the NEMD method, while different perturbations in the hot and sink sources is applied by the RNEMD method.

There are two kinds of methods in the RNEMD method, called the Müller-Plathe method [26] and the Jund method. The velocity of atoms in the hot and sink sources is exchanged by the Müller-Plathe method [29]. The energy in the hot and sink sources is exchanged by the Jund method.

In the application of the RNEMD method, the effects of material morphology, temperature, and irradiation on the thermal conductivity of SiC have been paid much attention. Qin et al. [26] used the Müller-Plathe method to calculate the thermal conductivity of SiC nanotubes. The coupling effects of the length, diameter, and temperature on the

thermal conductivity of SiC nanotubes were revealed. Mao et al. [27] used the quantum corrected Müller-Plathe method to calculate the thermal conductivity of 3C-SiC. The effects of the point defect type and the concentration on thermal conductivity were revealed. Dong et al. [29] used the Jund method to calculate the thermal conductivity of SiC/SiC composites. The effects of the irradiation dose and temperature on the change of thermal conductivity were revealed.

In the application of the NEMD method, the effects of material structure, temperature, and irradiation on the thermal conductivity of SiC have been paid much attention. Liu et al. [30] successfully studied the effect of different SiC crystal/amorphous layered nanostructures on the interfacial thermal conductivity. Wang et al. [28] revealed the effects of temperature and irradiation on the thermal conductivity of 3C-SiC.

In the application of the EMD method, the effects of irradiation and defects on the thermal conductivity of SiC have been paid much attention. Samolyuk et al. [31] revealed the effect of single vacancy and small vacancy clusters/micropores generated by irradiation on the thermal conductivity of 3C-SiC. Wang et al. [32] successfully studied the effects of types of point defects on the thermal conductivity of 3C-SiC.

3.1.2. MD Simulation Studies of SiC Mechanical Properties

Mechanical properties are important parameters affecting the processing performance and performance of SiC materials, and are one of the hotspots in the MD simulation studies of SiC properties. Various mechanical properties of SiC, such as hardness, elastic modulus, strength, etc., can be well calculated and analyzed at the nanoscale by MD simulation. Uniaxial tensile/compression and nanoindentation are two common methods used in MD studies of the mechanical properties of SiC materials.

The typical mechanical properties calculation model of SiC was given, as shown in Figure 3. The tension/pressure to both ends of the sample in a certain direction at the same time is applied by uniaxial tensile/compression, while the loading-unloading process of the indenter on the sample surface is controlled by nanoindentation.

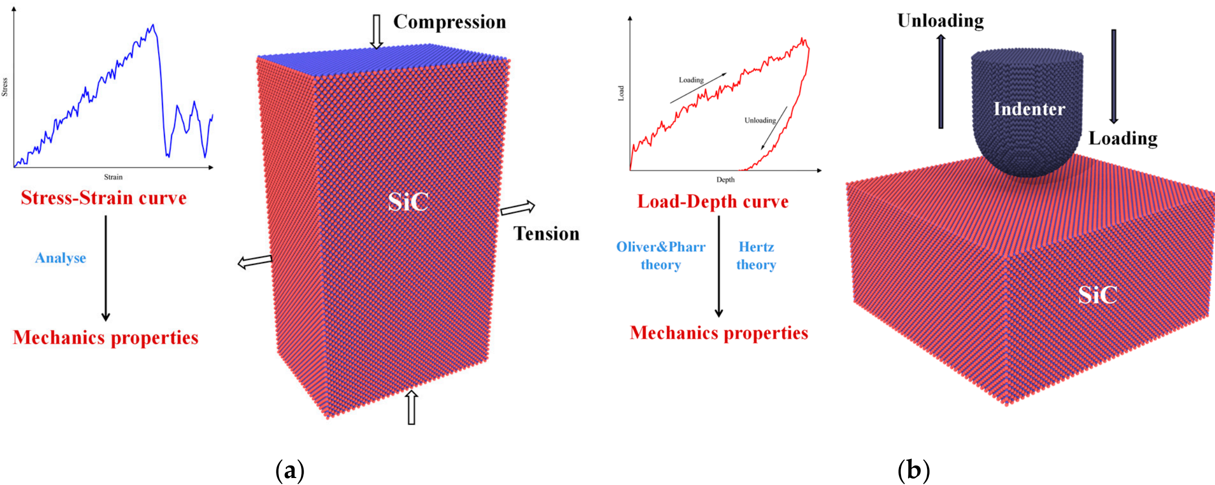

Figure 3. The typical mechanical properties calculation model of SiC: (**a**) Uniaxial tensile/compression; (**b**) Nanoindentation [33,34].

In the application of the uniaxial tensile/compressive, the tensile/compressive strength is usually calculated by analyzing the stress-strain curve. Yang et al. [35] calculated the tensile/compressive strength by calculating the stress-strain curve. The temperature dependence of the tensile/compressive strength of polycrystalline SiC was studied. Li et al. [36] calculated the tensile strength by the same method. The effects of irradiation and grain boundary on the tensile strength of 3C-SiC were studied. Molaei et al. [37] calculated the tensile strength and elastic modulus by analyzing the stress-strain behavior in the uniaxial

tension, based on the virial stress criterion. The effects of the temperature and the crack on the mechanical properties of polycrystalline SiC nanosheets were studied.

In the application of the nanoindentation, the hardness and elastic modulus are usually calculated by analyzing the load-depth curve, based on the Oliver and Pharr theory or Hertz theory. Wu et al. [38] calculated the hardness and elastic modulus using the Oliver and Pharr theory. The effects of Si ion implantation on the mechanical properties of 3C-SiC were studied successfully. Kang et al. [39] studied the effects of H ion implantation and temperature on the hardness and elastic modulus of 4H-SiC by the same method. Xue et al. [40,41] calculated the hardness and elastic modulus based on the Oliver and Pharr theory and Hertz theory. The effects of the temperature and indentation plane on the mechanical properties of 4H-SiC were studied.

3.1.3. MD Simulation Studies of SiC Electrical Properties

The electrical properties of SiC can be calculated by the MD method. For example, Domingues et al. [42] calculated the frequency-dependent dielectric constant based on the linear response theory and the Lorentz model. The effects of the temperature on the dielectric constant of SiC were revealed. Chen et al. [43] calculated the frequency-dependent dielectric constant of SiCm based on the linear response theory. The feasibility of combining deep neural networks with the MD method was demonstrated.

In general, there are few reports on the MD simulation of the electrical properties of SiC. Because there are few universal models for the correlation between microscopic information and macroscopic electrical characteristic parameters of MD simulation, it is worthy of further study.

3.2. MD Simulation Studies of Silicon Carbide Preparation

3.2.1. MD Simulation Studies of SiC Ion Implantation

Ion implantation is a method of surface modification by irradiating an ion beam into the surface of a solid material. It is widely applied in the element doping processing of semiconductor materials, such as SiC. A certain dose of the incident ion is injected into the material surface with a certain energy at a certain height from the surface of SiC materials to simulate the ion implantation process in the MD simulation. The typical ion implantation simulation model of SiC was given, as shown in Figure 4. There are three kinds of ion implantation in MD simulation studies of SiC according to the type of the implanted ion, called Si ion implantation, H ion implantation, and metal ion (Ga^{+}, Cu^{2+}, etc.) implantation. The effects of ion implantation on the defect evolution, mechanical properties, and processing properties of SiC materials can be studied by MD simulation.

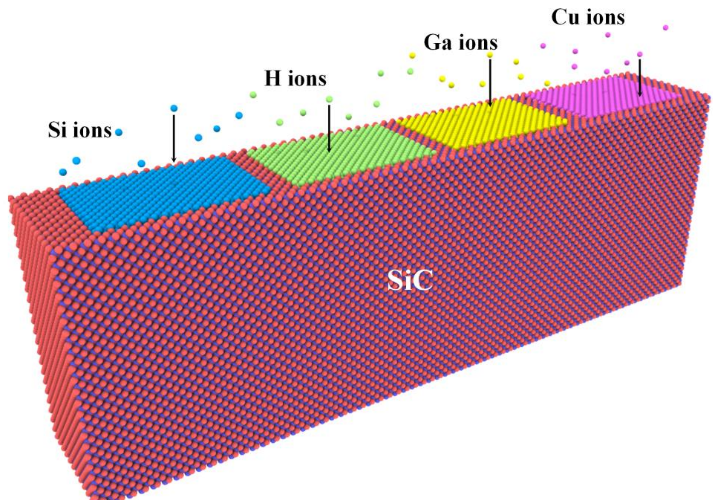

Figure 4. The typical ion implantation simulation model of SiC [44,45].

In the studies of Si ion implantation, Wu et al. [38] studied the effects of Si ion implantation dose and energy on the defect evolution and mechanical properties of 3C-SiC. Dai et al. [46] studied the effects of Si ion implantation energy on the 3C-SiC polishing effect. Liu et al. [47] studied the effects of Si ion implantation on the polishing removal mechanism of 6H-SiC. The studies showed that the hardness and elastic modulus of SiC could be reduced, the formation of dislocations in SiC could be inhibited, and the polishing performance and processing efficiency of SiC could be improved by Si ion implantation.

In the studies of H ion implantation, Fan et al. [48] studied the evolution mechanism of Si vacancy defects and damages during H ion implantation and the subsequent annealing of 4H-SiC. Kang et al. [39] studied the effects of H ion implantation on the mechanical properties of 4H-SiC. The studies showed that the integrity of Si vacancy defects in SiC could be improved, the crack propagation in SiC could be prevented, and the fracture toughness of SiC could be improved by H ion implantation.

In the studies of metal ion implantation, Fan et al. [44] studied the effects of the Ga ion implantation dose on the polishing effects of 4H-SiC. There are also studies on the synergistic implantation of metal ions and H ions. Kang et al. [49] studied the effects of the Cu ion assisted H ion on the modification of 4H-SiC. The studies showed that the ductility and surface toughness of SiC could be improved by metal ion implantation, and the synergistic ion implantation was more effective.

3.2.2. MD Simulation Studies of SiC Polishing

Polishing is an important process in the manufacturing process of SiC materials. There are three kinds of polishing in MD simulation studies of SiC according to the processing method, called abrasive polishing, tool polishing, and assisted polishing. The typical polishing simulation model of SiC was given, as shown in Figure 5. The removal and deformation mechanism of SiC material surface could be studied by MD simulation.

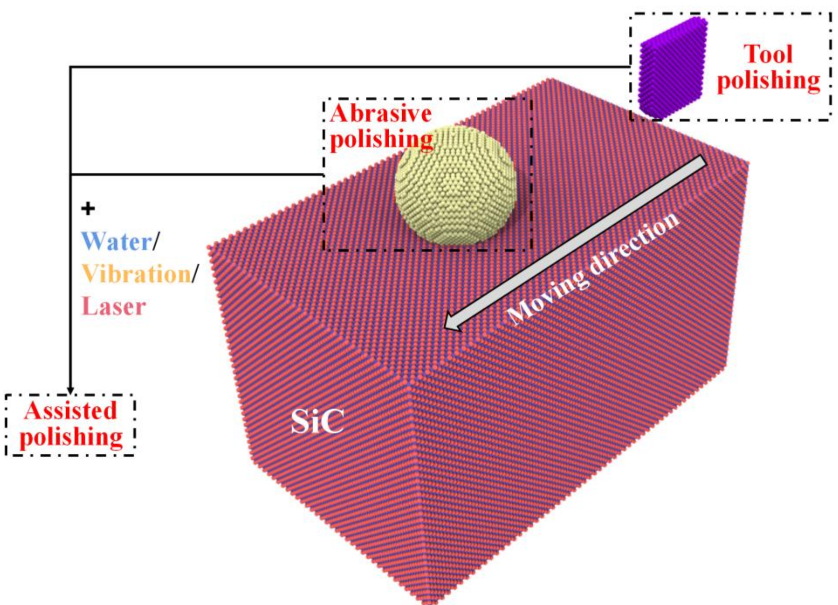

Figure 5. The typical polishing simulation model of SiC [50].

The surface of SiC materials is polished by spherical diamond abrasives in the abrasive polishing. In the studies of abrasive polishing, the removal mechanism has been paid much attention. Zhou et al. [51] studied the effects of multi-abrasive polishing on the removal mechanism of the 3C-SiC substrate. Wu et al. [52] studied the effects of abrasive size on the removal mechanism of 6H-SiC polishing. Zhou et al. [53] studied the effect of abrasive contact type on the removal mechanism of 3C-SiC polishing. The studies showed that the processing quality could be deteriorated by the random distribution of the abrasive. The

type of removal mechanism could be affected by the size of the abrasive, and the damages of the abrasive could be reduced by the rotation.

The surface of SiC materials is polished by sharp diamond tools in tool polishing. In the studies of tool polishing, the removal and deformation mechanism have been paid much attention. Meng et al. [54] studied the effects of polishing speed and thermal effect on the removal mechanism of 3C-SiC. Luo et al. [55] studied the effects of polishing depth and uniformity on the removal mechanism of 6H-SiC. Zhang et al. [56] studied the effects of the tool inclination angle on the deformation mechanism of 6H-SiC. Meng et al. [57] studied the effects of polishing direction on the deformation mechanism of 3C-SiC. Chavoshi et al. [58] studied the deformation mechanism of 3C-SiC polishing on different crystal orientations. The studies showed that the tool wear could be reduced by the thermal effect caused by high-speed polishing, the removal mechanism of SiC could be controlled by changing the cutting depth and uniformity, and the deformation mechanism of SiC could be controlled by changing the cutting direction and tool inclination angle.

The abrasive or tool polishing performance of SiC is improved by the supplementary method in assisted polishing. In the studies of assisted polishing, the removal and deformation mechanism have been paid much attention. Zhou [59] studied the effects of water-assisted polishing on the removal mechanism of 3C-SiC. Nguyen et al. [60] studied the effects of abrasive motion on the removal mechanism of 4H-SiC polishing. Hu et al. [61] studied the effect of vibration-assisted polishing on the removal mechanism of the single crystal SiC. Zhao et al. [62] studied the effect of ultrasonic vibration-assisted polishing on the deformation mechanism of 3C-SiC. Meng et al. [63] studied the effect of femtosecond laser-assisted polishing on the removal mechanism of 3C-SiC. The studies showed that the removal efficiency, surface finish, and integrity of SiC could be improved by assisted polishing.

3.2.3. MD Simulation Studies of SiC Sputtering

Sputtering is an important process in the manufacturing of semiconductor materials, such as SiC. It is applied to fabricate the required micro-nano structures on the surface of materials. There are two kinds of sputtering in MD simulation studies of SiC according to the incident substances, called inert substances sputtering and reactive substance sputtering. The typical sputtering simulation model of SiC was given, as shown in Figure 6. The sputtering mechanism, sputtering yield, and sputtering products on surface can be studied by MD simulation.

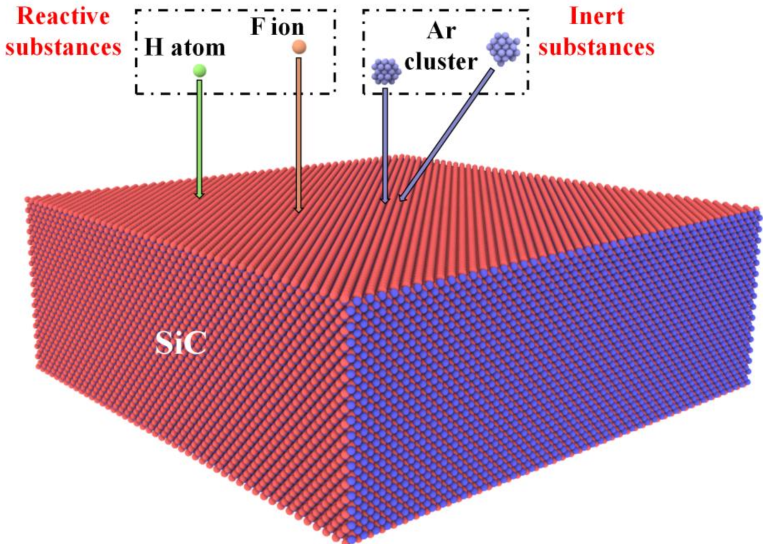

Figure 6. The typical sputtering simulation model of SiC [64,65].

In the studies of inert substances sputtering, Satake [64] studied the transverse sputtering mechanism caused by the collision of two Ar clusters on the surface of 4H-SiC. Prskalo et al. [66] studied the sputtering yield of the Ar atom sputtering the 3C-SiC surface. The studies showed that the surface modification effect of Ar atoms on SiC is obvious. The sputtering yield of SiC is a function of the incident energy of Ar atoms.

In the studies of reactive substances sputtering, Sun et al. [67] studied the effects of the incident energy of the H atom on the sputtering products of the continuous bombardment of the SiC surface by the H atom. Gou et al. [68] studied the effects of incident energy of CF_3 on the sputtering products of continuous bombardment of the SiC surface by CF_3. Lu et al. [69] studied the effect of the substrate temperature on the sputtering products of continuous bombardment of the SiC surface by the F ion. The studies showed that the thickness of the reaction layer, the composition, and yield of the sputtering product could be affected by the incident energy and substrate temperature.

3.2.4. MD Simulation Studies of SiC Deposition

The thin film deposition is one of the necessary steps in the manufacture of semiconductor materials, such as SiC. The typical deposition simulation model of SiC was given, as shown in Figure 7. The region deposited in the model is called the substrate. A number of Si atoms and C atoms are randomly generated in a region above the substrate. They fall and cover the substrate to form a SiC deposited layer. The effects of the atomic incident energy, substrate morphology, and substrate temperature on the quality of the SiC deposited films can be studied by MD simulation.

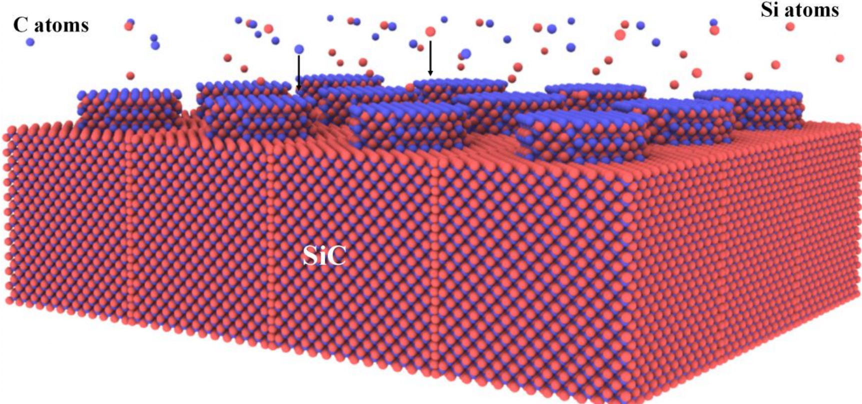

Figure 7. The typical deposition simulation model of SiC [70,71].

Xue et al. [70] studied the effects of the substrate pattern on SiC films deposited on 4H-SiC substrates. Kim et al. [72,73] studied the effects of the substrate temperature and atomic incident energy on the deposition of amorphous SiC films on crystalline silicon substrates. The studies showed that the chemical order of the deposited films can be controlled by adjusting the atomic incident energy, substrate morphology, and substrate temperature to obtain high-quality SiC films with dense and defect-free content.

3.2.5. MD Simulation Studies of SiC Crystal Growth

The high-quality growth of SiC crystals is the basis for manufacturing high-performance devices as an important semiconductor material. Fewer defects and higher density are usually required in SiC crystals. The typical crystal growth simulation model of SiC was given, as shown in Figure 8. Solid crystal SiC and liquid amorphous SiC are set in the model, and then the crystal growth process on the solid-liquid interface can be observed. The crystallization behavior and mechanism of SiC can be studied by MD simulation.

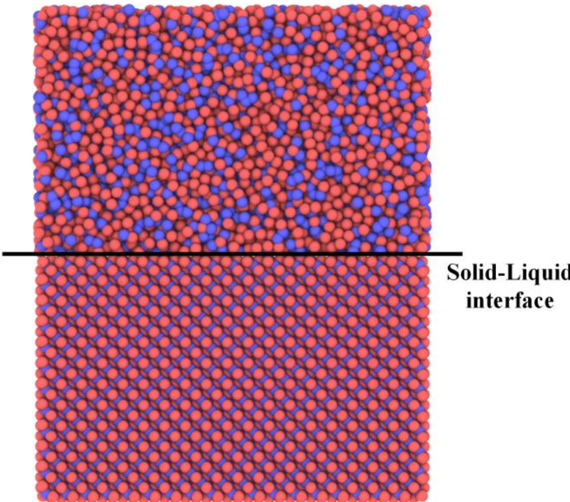

Figure 8. The typical crystal growth simulation model of SiC [74].

Narumi et al. [75] studied the effects of the growth interface on the growth behavior of 4H-SiC in the Si-C solution. Gao et al. [74] studied the crystallization behavior induced by SiC crystals at the solid-liquid interface. Kang [19] studied the effect mechanism of process variables on the formation of polymorphs in SiC single crystal growth. Gao et al. [21] studied the mechanism of the amorphous to the crystalline transition of 3C-SiC. The studies showed that the crystal growth rate and growth mechanism of SiC are different at different growth interfaces. The atoms near the growth interface tend to induce further crystallization by forming a stable intermediate-phase crystal structure.

3.2.6. MD Simulation Studies of SiC Amorphization

The preparation of SiC amorphous materials is also studied widely in the MD simulation of SiC preparation. There are two kinds of amorphization in MD simulation studies of SiC, called heating amorphization and cooling amorphization. The SiC material is heated from a low temperature above its melting point and melts into an amorphous material in the heating amorphization. The high-temperature molten SiC is rapidly cooled to low temperatures to form amorphous materials in the cooling amorphization. The typical amorphization simulation model of SiC was given, as shown in Figure 9. The structural evolution and mechanism of SiC amorphization can be studied by MD simulation.

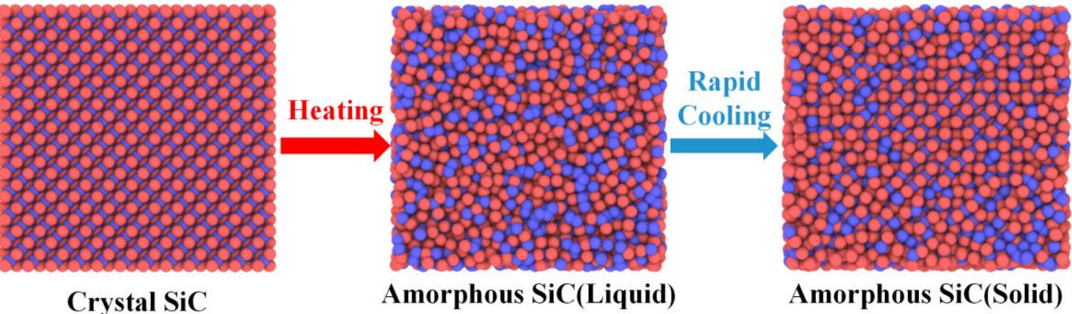

Figure 9. The typical amorphization simulation model of SiC [76,77].

In the studies of heating amorphization, Nguyen et al. [76] studied the structural evolution of SiC nanosheets during melting. Hoang et al. [78] studied the melting mechanism of two-dimensional (2D) hexagonal SiC nanoribbons. The studies showed that the liquid atoms in SiC first appear in the edge region of the material far below the melting point and then gradually expand to other regions.

In the studies of cooling amorphization, Tranh et al. [77] studied the effect of the potential function on the formation of glassy SiC nanoribbons by rapid cooling of molten SiC. Hoang et al. [79] studied the formation mechanism of the atomic structure of amorphous 2D SiC nanobelts obtained by cooling from melts. The studies showed that the Tersoff potential is more suitable for the simulation of cooling amorphization. The disordered atomic structure of amorphous 2D SiC nanoribbons is caused by various structural defects and the non-alternating distribution of Si and C atoms.

3.2.7. MD Simulation Studies of SiC Sintering

Sintering is an important preparation method of SiC materials and plays an important role in nuclear fuel study. For example, the matrix material of the fully ceramic microencapsulated accident-tolerant fuel (FCM-ATF) is made of SiC powder or nanoparticles. The typical sintering simulation model of SiC was given, as shown in Figure 10. Two SiC nanoparticles were placed in the cutoff distance of the potential function, then the system was heated to make the two particles contact each other and form a sintering neck, and finally completely sintered. The sintering process and mechanism of SiC nanoparticles from the microscopic view can be studied by MD simulation.

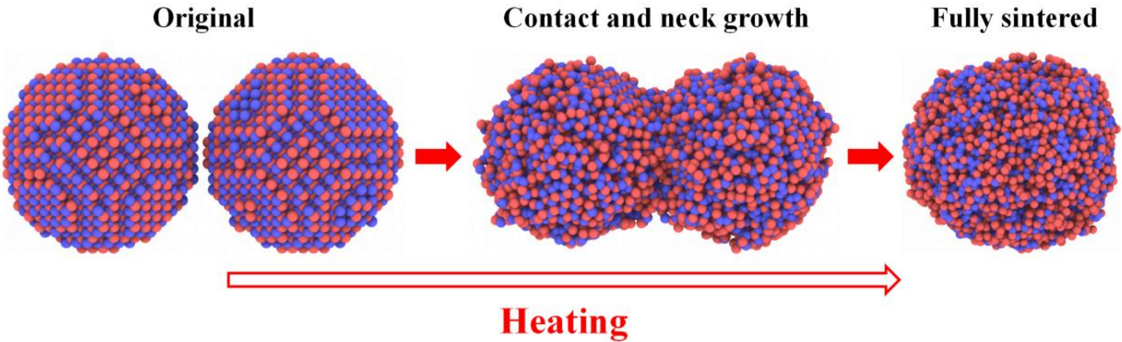

Figure 10. The typical sintering simulation model of SiC [80].

There are few related studies. Our research group conducted a preliminary study on MD simulation of SiC nanoparticle sintering recently. The sintering evolution and mechanism of three typical SiC nanoparticles: pure SiC, SiC@Si, and SiC@C were studied. The studies showed that the overall sintering behavior of SiC particles was promoted by the atomic diffusion of the coating layer. The lower heating rate is beneficial to sintering to some extent but did not affect the atomic diffusion mode of the coating particles.

3.2.8. MD Simulation Studies of New-Type SiC Materials Preparation

In addition to conventional SiC films, SiC bulks, and SiC crystals/amorphous materials, there are also some newly discovered SiC materials emerging in the MD simulation of SiC preparation. The preparation method of new-type SiC materials, such as nanowires and nanotubes can also be studied by MD simulation. SiC nanocage is expected to be an ideal material for drug delivery as a kind of new material. However, it is still in the conceptual stage. Its properties and the feasibility of preparation can be studied by the MD method.

Xin et al. [81] studied the existence, stability, and structure of Si_mC_n nanocages (Figure 11). A series of self-assembled, stable SiC nanocage structural materials were predicted successfully, and the key factors for the preparation of these new materials were studied.

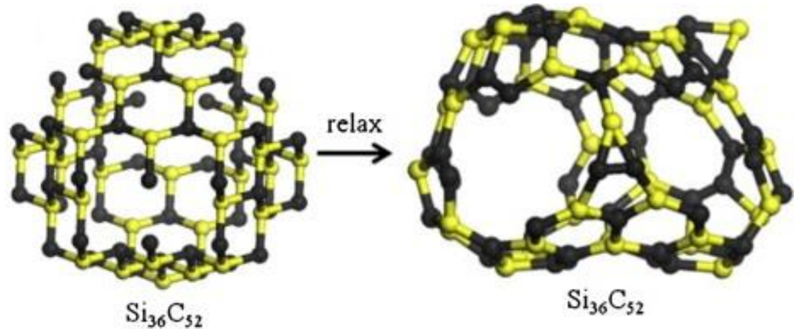

Figure 11. The formation process of a SiC nanocage in MD simulation, modified picture of [81].

3.3. MD Simulation Studies of Silicon Carbide Performance

3.3.1. MD Simulation Studies of SiC Irradiation Damage

The defects in materials will be produced by the impact of ray particles (neutrons, protons, heavy ions, electrons, X-rays, γ-rays), and the transmutation elements will be produced by the nuclear reactions. The change of macroscopic properties of materials caused by lattice defects and transmutation elements is called the irradiation effect. SiC is a kind of common nuclear material in advanced nuclear energy systems, and its irradiation process and effect are the key to the studies of performance. Therefore, the studies of irradiation damage have become the most concerned in the MD simulation of SiC performance.

There are three methods to simulate SiC irradiation damage in MD simulation. The first is to artificially remove some atoms in the material to form defects and simulate the damage effect after irradiation. The second is to use high-energy ray particles to impact materials to cause a cascade effect. The third is to choose an atom in the material and give it high energy to become a primary knock-on atom (PKA) to cause a cascade effect. The typical irradiation damage simulation model of SiC was given, as shown in Figure 12.

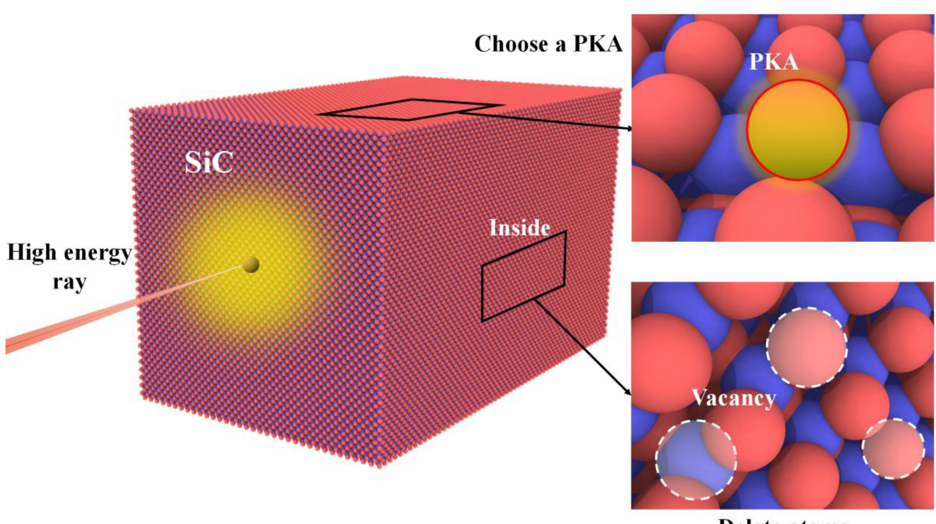

Figure 12. Three typical irradiation damage simulation models of SiC [82].

There are two main concerns in the content of MD simulation studies of SiC irradiation damage. The first is the effects of irradiation on properties. The second is the mechanism of irradiation damage, as shown in Figure 13.

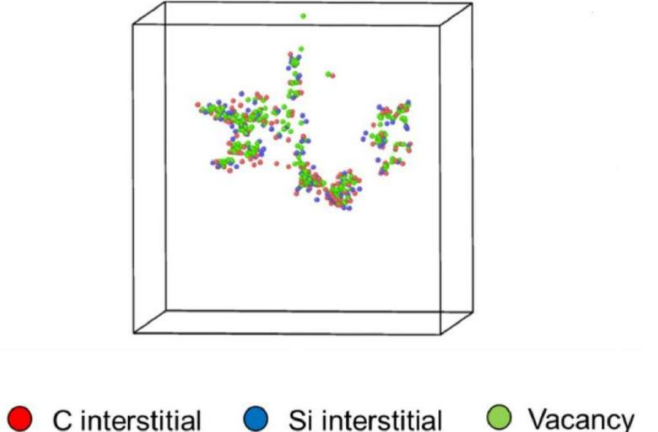

Figure 13. The typical irradiation damage mechanism simulation model of SiC, modified picture of [28].

To sum up, there are two aspects in MD simulation studies of the effects of irradiation on SiC properties. The first is the effects of irradiation on the thermal properties of SiC (mainly the thermal conductivity). Wang et al. [28] studied the effects of irradiation on the thermal conductivity of 3C-SiC by simulating the irradiation effect with high-energy Si atoms and subsequent cascade collisions. Nguyen et al. [83] studied the relationship between defect thermal conductivity and vacancy concentration and irradiation dose by calculating the thermal conductivity of SiC/SiC composites under neutron irradiation. Samolyuk et al. [31] studied the effects of irradiation-induced single vacancy and small vacancy clusters/micropores on the thermal conductivity of 3C-SiC. Dong et al. [29] studied the effects of the irradiation-induced point defects at the interface of SiC/SiC composites and the irradiation dose on the thermal conductivity. The studies showed that the thermal conductivity of SiC could be decreased by irradiation damage. The thermal conductivity of SiC could be decreased more by a single vacancy than a micropore with the same total number of vacancies.

The second is the effects of irradiation on the mechanical properties of SiC. Li et al. [36] studied the effects of irradiation on the tensile strength and elastic modulus of 3C-SiC. The studies showed that the tensile strength and elastic modulus of 3C-SiC could be decreased by irradiation damage.

To sum up, there are three aspects in MD simulation studies of the mechanism of SiC irradiation damage. The first is the formation process and mechanism of irradiation defects. Zarkadoula et al. [84] studied the effects of the electron blocking power on defects in 3C-SiC caused by ion irradiation. Samolyuk et al. [85] studied the effects of potential functions on defects in 3C-SiC collision cascade simulation. He et al. [86] studied the formation of defects and the effects of electron energy loss during the irradiation damage of SiC materials. Wu et al. [82] studied the fast, ion-induced effects in 3C-SiC and the effects of the complex correlation between the electronic response and atomic response on the defect formation. Li et al. [87] studied the irradiation damage mechanism of 6H-SiC under ultra-high flux He ions. Ran et al. [88] studied the effects of temperature and PKA energy on collision cascade in 3C-SiC. The studies showed that the formation of irradiation defects was affected importantly by the ratio of electron energy loss to nuclear energy loss. The number and size of defects increased with the increase in PKA energy.

The second Is the recovery mechanism of irradiation defects. Backman et al. [89] studied the defect recovery of irradiated SiC under fast, heavy ion irradiation. Peterson et al. [90] studied the effects of high field bias on the irradiation-induced defect recovery in 3C-SiC. The studies showed that the defects could be recovered by the heavy ion rapid annealing. The defect recovery effect could be enhanced by the field strength lower than the critical breakdown of the wide band gap device.

The third is the formation mechanism of irradiation swelling. Li et al. [91] studied the effect of the C/Si atomic ratio on the irradiation swelling of 3C-SiC. Tian et al. [92] studied the swelling of SiC crystals caused by continuous collision cascades at room temperature. The studies showed that the degree of irradiation swelling decreased with the increase in the C/Si ratio in SiC. The amorphization of SiC could be caused by the irradiation swelling. There are four stages of amorphization, called slow increase, rapid increase, slow increase, and completely amorphous.

3.3.2. MD Simulation Studies of SiC Fatigue Damage

A crack is a kind of fatigue damage caused by local fracture of the weak part of material under force. SiC maybe cracks when applied as a structural material if the tension exceeds a certain value. The typical fatigue damage simulation model of SiC was given, as shown in Figure 14. The atoms in certain fields are removed artificially during the material modeling to form initial cracks, then an external force is applied to the material. The evolution of cracks in SiC under external force and its effect on SiC mechanical properties can be studied by MD simulation.

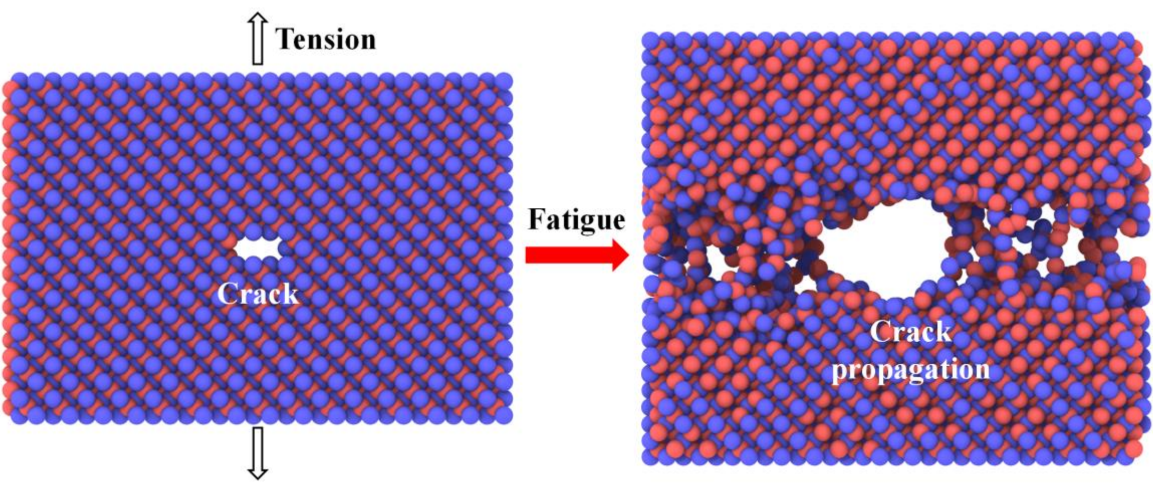

Figure 14. The typical fatigue damage simulation model of SiC [93].

Molaei et al. [37] studied the fracture fingerprint of polycrystalline SiC nanosheets with single crystalline SiC nanosheets as reference. The study showed that the properties of SiC nanosheets with cracks could be degraded with the increase in temperature. The strength of SiC nanosheets was reduced seriously by the large cracks.

3.3.3. MD Simulation Studies of SiC Shock Damage

SiC will be subjected to sudden mechanical action when applied as a protective material. For example, SiC is shocked by high-speed moving objects when it is applied as bulletproof materials. The typical shock damage simulation model of SiC was given, as shown in Figure 15. The shock waves are created by hitting SiC samples with a high-velocity virtual piston to result in damage effects. The effects of shock velocity on the shock response to SiC can be studied by MD simulation.

Feng et al. [94] studied the inelastic response to 6H-SiC and 4H-SiC under strong dynamic shock loading. Lee et al. [95] studied the high-velocity shock compression of 3C-SiC. Zhang et al. [96] studied the shock profile and atomic structure evolution of 3C-SiC under plane shock loading. These studies showed that different response states in SiC could be produced with the change of shock velocity, such as the single elastic wave, structural phase transition wave, etc.

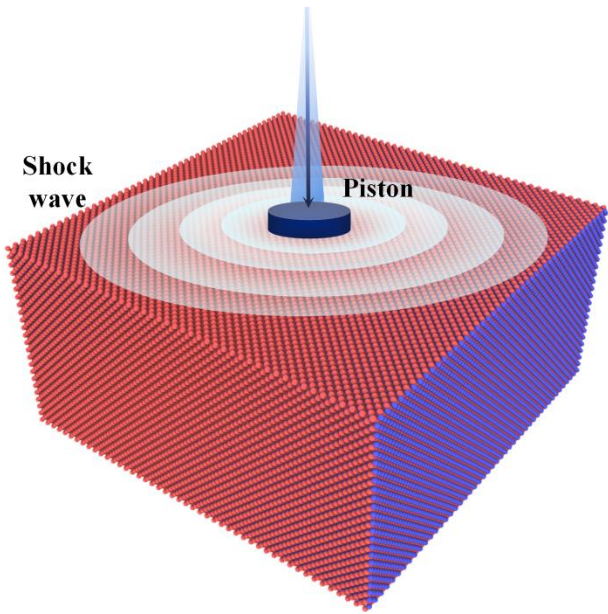

Figure 15. The typical shock damage simulation model of SiC [94].

4. Conclusions

The SiC materials are the current study hotspots as the fourth-generation nuclear materials and the third-generation semiconductor materials. The extensive studies on the MD simulation of SiC materials are summarized, as shown in Figure 16.

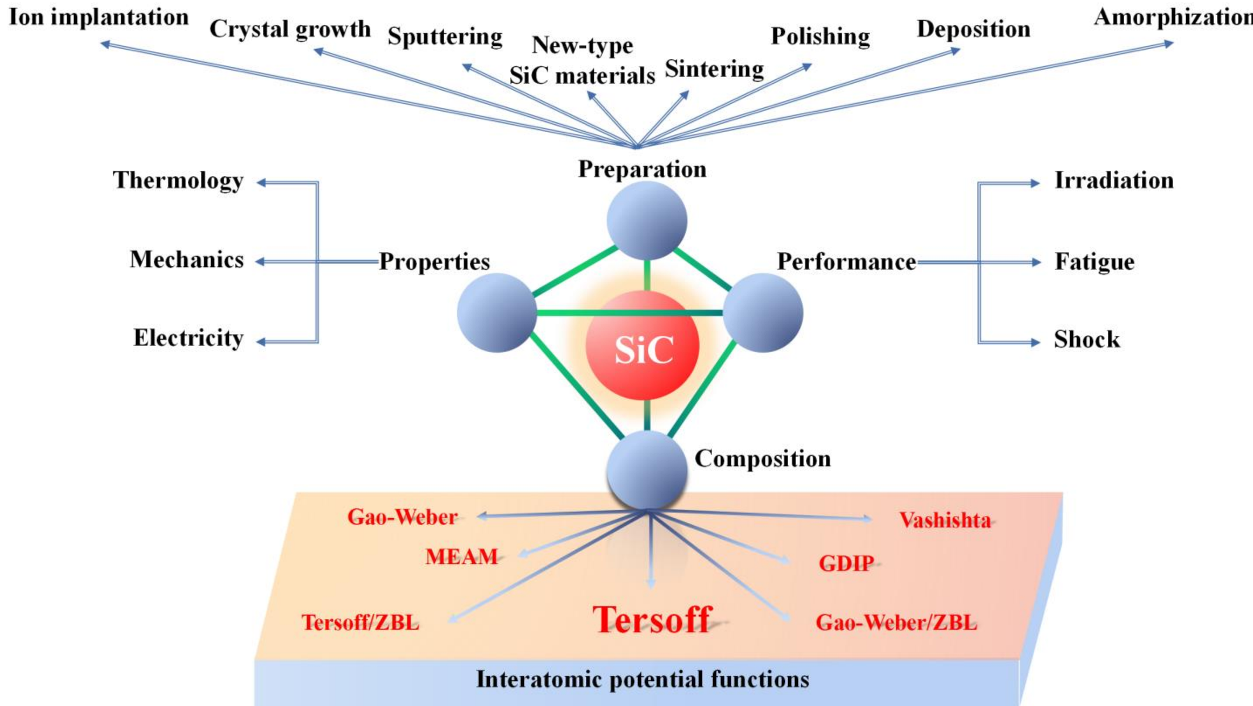

Figure 16. The brief summary of MD simulation studies of SiC materials.

In this paper, the comparison study of interatomic potential function for SiC MD simulation are given, and advances in the MD simulation studies of properties, preparation, and performance of SiC materials were systematically summarized. The conclusions can be obtained as follows:

(1) The Tersoff potential was the most popular interatomic potential function for SiC materials because it provided a satisfactory balance between computational accuracy and computational speed. Most of the MD simulation types in the properties, preparation, and properties of SiC materials were covered in the application scope of the Tersoff potential.
(2) In the MD simulations of SiC materials' properties, the thermal and mechanical properties, such as thermal conductivity, hardness, elastic modulus, etc., were studied mostly due to the limitation of the study scale. At present, mature simulation calculation methods were formed, and simulation results similar to the experimental measurements could be obtained.
(3) In the MD simulations of SiC material's preparation, ion implantation, polishing, sputtering, deposition, crystal growth, etc., were mainly studied. Most of these preparation methods were closely related to semiconductor fabrication processes and well-matched the nanoscale accuracy of semiconductor fabrication. The mechanism and quality in the preparation of SiC materials were mainly focused to obtain the guidance of preparation process optimization.
(4) In the MD simulations of SiC materials performance, the irradiation damage was studied mostly. There are also some studies on the fatigue damage and impact damage. These studies are closely related to the performance of SiC materials in the field of nuclear energy. The effects of various damages (especially irradiation damage) on the properties of SiC materials during service, as well as the process and mechanism of damage, could be revealed by MD simulation from the atomic-level microscopic perspective. The theoretical guidance for the design optimization of SiC materials for nuclear energy and the improvement of nuclear reactor safety could be obtained.

5. Prospect of Future Study

The MD simulation of SiC materials has been successfully applied in the field of nuclear energy and semiconductors, and has been studied as structural materials (backing materials) functional materials (thermally conducting material, protective materials), etc. However, there are still many specific study areas that have not been fully developed. The demand for MD simulation is bound to increase with the deepening of the experimental study on SiC materials. Therefore, the aspects worthy of great attention in the future MD simulation of SiC materials are recommended as follows:

(1) In the preparation of SiC materials, including the chemical vapor deposition, sintering, and embedding solid phase reaction preparation of SiC are common methods of nuclear fuel preparation. For example, in the fourth-generation nuclear energy system, SiC can be applied as the cladding material of tri-structural iso-tropic (TRISO) fuel or the matrix material of FCM-ATF. The former is prepared by fluidized bed chemical vapor deposition (FB-CVD) technology, and the latter is prepared by powder sintering. Therefore, it is necessary to strengthen the study on CVD and nanoparticle sintering in the MD simulation of SiC materials preparation. The appropriate microscopic process parameters to characterize the preparation process are necessary to find. They should be linked with the macroscopic parameters to provide reference and guidance for the preparation process optimization of nuclear fuel and SiC ceramics.
(2) In the MD simulation of SiC properties, the accuracy of the simulation of thermal and mechanical parameters should be focused on. The development of the MD potential function and the accuracy of potential function parameters is involved. In the MD simulation study of SiC materials, the potential function is the basis and key aspect. The parameter optimization and verification, based on the existing potential functions of SiC, are necessary to strengthen to ensure the accuracy of the simulation results of properties, preparation, and properties. In addition, most of the current MD simulations of SiC materials stay at the level of physical phenomena but rarely involve chemical reactions. Therefore, the reactive force-field (ReaxFF) MD study and the development of ReaxFF potential for SiC materials is necessary to

strengthen. It is particularly helpful for the preparation and performance simulation closer to reality. More importantly, more suitable potential functions for specific fields, environments, and purposes are needed to be developed. The microscopic and macroscopic connection parameters are necessary to develop, in particular. It means parameters that are more helpful for macroscopic experimental verification, such as melting point, elastic modulus, and Poisson's ratio, etc., are obtained from the MD microscopic simulation results.

(3) In the MD simulation of the SiC performance, there are many more scenarios that should be considered. The nuclear energy field (multiple ray collaborative irradiation), the semiconductor field (precision manufacturing, threshold characteristics), the bulletproof material field (mechanical shock), the chemical environmental protection machinery field (corrosion resistance, high-temperature resistance), etc., are included. It should be noted that the MD simulation of irradiation damage has been well studied and developed as a typical application scenario in the field of nuclear energy. However, more influencing factors should be considered to make the study closer to the real reactor environment and strengthen the verification of experimental results.

Author Contributions: Methodology, investigation, writing—original draft preparation, Z.Y.; conceptualization and method discussion, R.L.; resources, B.L.; data curation, Y.S.; conceptualization, writing—review and editing, supervision, M.L. All authors have read and agreed to the published version of the manuscript.

Funding: This research was funded by National Youth Talent Support program (grant number 20224723061) and National Major S&T project (grant number ZX06901).

Data Availability Statement: Not applicable.

Acknowledgments: Thanks to the open-source software, LAMMPS and OVITO.

Conflicts of Interest: The authors declare no conflict of interest.

References

1. Liu, R.Z.; Liu, B.; Zhang, K.H.; Liu, M.L.; Shao, Y.L.; Tang, C.H. High temperature oxidation behavior of SiC coating in TRISO coated particles. *J. Nucl. Mater.* **2014**, *453*, 107–114. [CrossRef]
2. Shi, L.; Zhao, J.Q.; Liu, B.; Li, X.W.; Luo, X.W.; Zhang, Z.M.; Zhang, P.; Sun, L.B.; Wu, X.X. Development strategy of key materials technology for the high temperature gas-cooled reactor. *J. Tsinghua Univ.* **2021**, *61*, 270–278. [CrossRef]
3. Terrani, K.A.; Kiggans, J.O.; Katoh, Y.; Shimoda, K.; Montgomery, F.C.; Armstrong, B.L.; Parish, C.M.; Hinoki, T.; Hunn, J.D.; Snead, L.L. Fabrication and characterization of fully ceramic microencapsulated fuels. *J. Nucl. Mater.* **2012**, *426*, 268–276. [CrossRef]
4. She, X.; Huang, A.Q.; Lucia, O.; Ozpineci, B. Review of Silicon Carbide Power Devices and Their Applications. *IEEE Trans. Ind. Electron.* **2017**, *64*, 8193–8205. [CrossRef]
5. Li, C.R.; Xie, Z.P.; Kang, G.X.; An, D.; Wei, H.K.; Zhao, L. Research and Application Progress of SiC Ceramics: A Review. *Bull. Chin. Ceram. Soc.* **2020**, *39*, 1353–1370. [CrossRef]
6. Zhai, F.R.; Shan, K.; Xie, Z.P.; Sun, J.L.; Yi, Z.Z. Preparation and Mechanical Properties of SiC/BN Multiphase Ceramics via Spark Plasma Sintering. *J. Chin. Ceram. Soc.* **2016**, *44*, 866–871. [CrossRef]
7. Li, C.R.; Xie, Z.P.; Zhao, L. Research and Application of Sintering Technologies for SiC Ceramic Materials: A review. *J. Ceram.* **2020**, *41*, 137–149. [CrossRef]
8. Thompson, A.P.; Aktulga, H.M.; Berger, R.; Bolintineanu, D.S.; Brown, W.M.; Crozier, P.S.; Veld, P.J.I.; Kohlmeyer, A.; Moore, S.G.; Nguyen, T.D.; et al. LAMMPS—A flexible simulation tool for particle-based materials modeling at the atomic, meso, and continuum scales. *Comput. Phys. Commun.* **2022**, *271*, 108171. [CrossRef]
9. Tersoff, J. New Empirical-Approach for the Structure and Energy of Covalent Systems. *Phys. Rev. B* **1988**, *37*, 6991–7000. [CrossRef]
10. Tersoff, J. Modeling Solid-State Chemistry: Interatomic Potentials for Multicomponent Systems. *Phys. Rev. B* **1989**, *39*, 5566–5568. [CrossRef]
11. Devanathan, R.; de la Rubia, T.D.; Weber, W.J. Displacement threshold energies in β-SiC. *J. Nucl. Mater.* **1998**, *253*, 47–52. [CrossRef]
12. Ziegler, J.F.; Biersack, J.P. The Stopping and Range of Ions in Matter. In *Treatise on Heavy-Ion Science: Volume 6: Astrophysics, Chemistry, and Condensed Matter*; Bromley, D.A., Ed.; Springer: Boston, MA, USA, 1985; pp. 93–129.
13. Vashishta, P.; Kalia, R.K.; Rino, J.P.; Ebbsjo, I. Interaction Potential for SiO2—A Molecular-Dynamics Study of Structural Correlations. *Phys. Rev. B* **1990**, *41*, 12197–12209. [CrossRef] [PubMed]
14. Vashishta, P.; Kalia, R.K.; Nakano, A.; Rino, J.P. Interaction potential for silicon carbide: A molecular dynamics study of elastic constants and vibrational density of states for crystalline and amorphous silicon carbide. *J. Appl. Phys.* **2007**, *101*, 103515. [CrossRef]

15. Bazant, M.Z.; Kaxiras, E.; Justo, J.F. Environment-dependent interatomic potential for bulk silicon. *Phys. Rev. B* **1997**, *56*, 8542–8552. [CrossRef]
16. Jiang, C.; Morgan, D.; Szlufarska, I. Carbon tri-interstitial defect: A model for the D-II center. *Phys. Rev. B* **2012**, *86*, 144118. [CrossRef]
17. Baskes, M.I. Modified Embedded-Atom Potentials for Cubic Materials and Impurities. *Phys. Rev. B* **1992**, *46*, 2727–2742. [CrossRef]
18. Huang, H.C.; Ghoniem, N.M.; Wong, J.K.; Baskes, M.I. Molecular-Dynamics Determination of Defect Energetics in β-SiC Using three Representative Empirical Potentials. *Model. Simul. Mater. Sc.* **1995**, *3*, 615–627. [CrossRef]
19. Kang, K.H.; Eun, T.; Jun, M.C.; Lee, B.J. Governing factors for the formation of 4H or 6H-SiC polytype during SiC crystal growth: An atomistic computational approach. *J. Cryst. Growth.* **2014**, *389*, 120–133. [CrossRef]
20. Gao, F.; Weber, W.J. Empirical potential approach for defect properties in 3C-SiC. *Nucl. Instrum. Meth. B* **2002**, *191*, 504–508. [CrossRef]
21. Gao, F.; Devanathan, R.; Zhang, Y.; Weber, W.J. Annealing simulations of nano-sized amorphous structures in SiC. *Nucl. Instrum. Meth. B* **2005**, *228*, 282–287. [CrossRef]
22. Tersoff, J. Carbon Defects and Defect Reactions in Silicon. *Phys. Rev. Lett.* **1990**, *64*, 1757–1760. [CrossRef] [PubMed]
23. Tersoff, J. Chemical Order in Amorphous-Silicon Carbide. *Phys. Rev. B* **1994**, *49*, 16349–16352. [CrossRef] [PubMed]
24. Erhart, P.; Albe, K. Analytical potential for atomistic simulations of silicon, carbon, and silicon carbide. *Phys. Rev. B* **2005**, *71*, 035211. [CrossRef]
25. Stillinger, F.H.; Weber, T.A. Computer-Simulation of Local Order in Condensed Phases of Silicon. *Phys. Rev. B* **1985**, *31*, 5262–5271. [CrossRef] [PubMed]
26. Qin, C.L.; Luo, X.Y.; Xie, Q.; Wu, Q.D. Molecular dynamics study of thermal conductivity of carbon nanotubes and silicon carbide nanotubes. *Acta Phys. Sin.* **2022**, *71*, 030202. [CrossRef]
27. Mao, Y.C.; Li, Y.Y.; Xiong, Y.H.; Xiao, W. Point defect effects on the thermal conductivity of β-SiC by molecular dynamics simulations. *Comput. Mater. Sci.* **2018**, *152*, 300–307. [CrossRef]
28. Wang, Q.; Gui, N.; Huang, X.L.; Yang, X.T.; Tu, J.Y.; Jiang, S.Y. The effect of temperature and cascade collision on thermal conductivity of 3C-SiC: A molecular dynamics study. *Int. J. Heat Mass Transf.* **2021**, *180*, 121822. [CrossRef]
29. Dong, X.Y.; Shin, Y.C. Predictions of thermal conductivity and degradation of irradiated SiC/SiC composites by materials-genome-based multiscale modeling. *J. Nucl. Mater.* **2018**, *512*, 268–275. [CrossRef]
30. Liu, Q.F.; Yu, W.S.; Luo, H.; Ren, X.; Shen, S.P. Tuning thermal resistance of SiC crystal/amorphous layered nanostructures via changing layer thickness. *Comput. Mater. Sci.* **2020**, *184*, 109868. [CrossRef]
31. Samolyuk, G.D.; Golubov, S.I.; Osetsky, Y.N.; Stoller, R.E. Molecular dynamics study of influence of vacancy types defects on thermal conductivity of β-SiC. *J. Nucl. Mater.* **2011**, *418*, 174–181. [CrossRef]
32. Wang, F.; Zhou, Y.; Gao, S.X.; Duan, Z.G.; Sun, Z.P.; Wang, J.; Zou, Y.; Fu, B.Q. Molecular dynamics study of effects of point defects on thermal conductivity in cubic silicon carbide. *Acta Phys. Sin.* **2022**, *71*, 036501. [CrossRef]
33. Zhang, B.Y.; Qiu, H.P.; Tian, Y.; Chen, M.W.; Chen, S.H. Tension-Tension Fatigue of 2.5D-SiC/SiC Ceramic Matrix Composites at Elevated Temperatures. *IOP Conf. Ser. Mater. Sci. Eng.* **2019**, *678*, 012057. [CrossRef]
34. Zhang, Z.Z.; Yao, P.; Wang, J.; Huang, C.Z.; Zhu, H.T.; Liu, H.L.; Zou, B. Nanomechanical characterization of RB-SiC ceramics based on nanoindentation and modelling of the ground surface roughness. *Ceram. Int.* **2020**, *46*, 6243–6253. [CrossRef]
35. Yang, B.; Deng, Q.B.; Su, Y.; Peng, X.H.; Huang, C.; Lee, A.; Hu, N. The effects of atomic arrangements on mechanical properties of 2H, 3C, 4H and 6H-SiC. *Comput. Mater. Sci.* **2022**, *203*, 111114. [CrossRef]
36. Li, Y.Y.; Li, Y.; Xiao, W. Point defects and grain boundary effects on tensile strength of 3C-SiC studied by molecular dynamics simulations. *Nucl. Eng. Technol.* **2019**, *51*, 769–775. [CrossRef]
37. Molaei, F.; Dehaghani, M.Z.; Salmankhani, A.; Fooladpanjeh, S.; Sajadi, S.M.; Safa, M.E.; Abida, O.; Habibzadeh, S.; Mashhadzadeh, A.H.; Saeb, M.R. Applying molecular dynamics simulation to take the fracture fingerprint of polycrystalline SiC nanosheets. *Comput. Mater. Sci.* **2021**, *200*, 110770. [CrossRef]
38. Wu, W.L.; Hu, Y.; Meng, X.S.; Dai, J.B.; Dai, H.F. Molecular dynamics simulation of ion-implanted single-crystal 3C-SiC nanoindentation. *J. Manuf. Process.* **2022**, *79*, 356–368. [CrossRef]
39. Kang, Q.; Fang, X.; Wu, C.; Verma, P.; Sun, H.; Tian, B.; Zhao, L.; Wang, S.; Zhu, N.; Maeda, R.; et al. Mechanical properties and indentation-induced phase transformation in 4H–SiC implanted by hydrogen ions. *Ceram. Int.* **2022**, *48*, 15334–15347. [CrossRef]
40. Xue, L.H.; Feng, G.; Liu, S. Molecular dynamics study of temperature effect on deformation behavior of m-plane 4H-SiC film by nanoindentation. *Vacuum* **2022**, *202*, 111192. [CrossRef]
41. Xue, L.H.; Feng, G.; Wu, G.; Dong, F.; Liang, K.; Li, R.; Wang, S.Z.; Liu, S. Study of deformation mechanism of structural anisotropy in 4H-SiC film by nanoindentation. *Mater. Sci. Semicond. Process.* **2022**, *146*, 106671. [CrossRef]
42. Domingues, G.; Monthe, A.M.; Guevelou, S.; Rousseau, B. Study by molecular dynamics of the influence of temperature and pressure on the optical properties of undoped 3C-SiC structures. *J. Quant. Spectrosc. Radiat. Transf.* **2018**, *205*, 220–229. [CrossRef]
43. Chen, W.; Li, L.S. The study of the optical phonon frequency of 3C-SiC by molecular dynamics simulations with deep neural network potential. *J. Appl. Phys.* **2021**, *129*, 244104. [CrossRef]
44. Fan, Y.X.; Xu, Z.W.; Song, Y.; Dong, B.; Xue, Z.F.; Liu, B.; Liu, L.; Tian, D.Y. Nano material removal mechanism of 4H-SiC in ion implantation-assisted machining. *Comput. Mater. Sci.* **2021**, *200*, 110837. [CrossRef]
45. Zhang, X.D.; Li, Q.; Wang, M.; Zhang, Z.T.; Akhmadaliev, S.; Zhou, S.Q.; Wu, Y.Y.; Guo, B. Defects in hydrogen implanted SiC. *Nucl. Instrum. Meth. B* **2018**, *436*, 107–111. [CrossRef]

46. Dai, H.F.; Hu, Y.; Wu, W.L.; Yue, H.X.; Meng, X.S.; Li, P.; Duan, H.G. Molecular dynamics simulation of ultra-precision machining 3C-SiC assisted by ion implantation. *J. Manuf. Process.* **2021**, *69*, 398–411. [CrossRef]
47. Liu, B.; Xu, Z.W.; Wang, Y.; Gao, X.; Kong, R.J. Effect of ion implantation on material removal mechanism of 6H-SiC in nano-cutting: A molecular dynamics study. *Comput. Mater. Sci.* **2020**, *174*, 109476. [CrossRef]
48. Fan, Y.X.; Xu, Z.W.; Song, Y.; Sun, T.Z. Molecular dynamics simulation of silicon vacancy defects in silicon carbide by hydrogen ion implantation and subsequent annealing. *Diam. Relat. Mater.* **2021**, *119*, 108595. [CrossRef]
49. Kang, Q.; Fang, X.D.; Wu, C.; Sun, H.; Tian, B.; Zhao, L.B.; Wang, S.L.; Jiang, Z.D.; Zhu, N.; Maeda, R.; et al. Modification mechanism of collaborative ions implanted into 4H-SiC by atomic simulation and experiment. *Int. J. Mech. Sci.* **2021**, *212*, 106832. [CrossRef]
50. Ma, G.L.; Li, S.J.; Liu, F.L.; Zhang, C.; Jia, Z.; Yin, X.C. A Review on Precision Polishing Technology of Single-Crystal SiC. *Crystals* **2022**, *12*, 101. [CrossRef]
51. Zhou, P.; Zhu, N.N.; Xu, C.Y.; Niu, F.L.; Li, J.; Zhu, Y.W. Mechanical removal of SiC by multi-abrasive particles in fixed abrasive polishing using molecular dynamics simulation. *Comput. Mater. Sci.* **2021**, *191*, 110311. [CrossRef]
52. Wu, Z.H.; Zhang, L.C.; Yang, S.Y.; Wu, C.H. Effects of grain size and protrusion height on the surface integrity generation in the nanogrinding of 6H-SiC. *Tribol. Int.* **2022**, *171*, 107563. [CrossRef]
53. Zhou, Y.Q.; Huang, Y.H.; Li, J.M.; Zhu, F.L. The effect of contact types on SiC polishing process. *Mater. Sci. Semicond. Process.* **2022**, *147*, 106709. [CrossRef]
54. Meng, B.B.; Yuan, D.D.; Xu, S.L. Study on strain rate and heat effect on the removal mechanism of SiC during nano-scratching process by molecular dynamics simulation. *Int. J. Mech. Sci.* **2019**, *151*, 724–732. [CrossRef]
55. Luo, Q.F.; Lu, J.; Tian, Z.; Jiang, F. Controllable material removal behavior of 6H-SiC wafer in nanoscale polishing. *Appl. Surf. Sci.* **2021**, *562*, 150219. [CrossRef]
56. Zhang, S.; Cheng, X.; Chen, J.Y. Surface deformation, phase transition and dislocation mechanisms of single crystalline 6H-SiC in oblique nano-cutting. *Appl. Surf. Sci.* **2022**, *588*, 152944. [CrossRef]
57. Meng, B.B.; Yuan, D.D.; Zheng, J.; Qiu, P.; Xu, S.L. Tip-based nanomanufacturing process of single crystal SiC: Ductile deformation mechanism and process optimization. *Appl. Surf. Sci.* **2020**, *500*, 144039. [CrossRef]
58. Chavoshi, S.Z.; Luo, X.C. Molecular dynamics simulation study of deformation mechanisms in 3C-SiC during nanometric cutting at elevated temperatures. *Mater. Sci. Eng. A-Struct.* **2016**, *654*, 400–417. [CrossRef]
59. Zhou, P.; Li, J.; Wang, Z.K.; Chen, J.P.; Li, X.; Zhu, Y.W. Molecular dynamics study of the removal mechanism of SiC in a fixed abrasive polishing in water lubrication. *Ceram. Int.* **2020**, *46*, 24961–24974. [CrossRef]
60. Nguyen, V.T.; Fang, T.H. Material removal and interactions between an abrasive and a SiC substrate: A molecular dynamics simulation study. *Ceram. Int.* **2020**, *46*, 5623–5633. [CrossRef]
61. Hu, Z.W.; Chen, Y.; Lai, Z.Y.; Yu, Y.Q.; Xu, X.P.; Peng, Q.; Zhang, L. Coupling of double grains enforces the grinding process in vibration-assisted scratch: Insights from molecular dynamics. *J. Mater. Process. Technol.* **2022**, *304*, 117551. [CrossRef]
62. Zhao, L.; Zhang, J.J.; Zhang, J.G.; Hartmaier, A. Atomistic investigation of machinability of monocrystalline 3C-SiC in elliptical vibration-assisted diamond cutting. *Ceram. Int.* **2021**, *47*, 2358–2366. [CrossRef]
63. Meng, B.B.; Yuan, D.D.; Zheng, J.; Xu, S.L. Molecular dynamics study on femtosecond laser aided machining of monocrystalline silicon carbide. *Mater. Sci. Semicond. Process.* **2019**, *101*, 1–9. [CrossRef]
64. Satake, S.; Yamashina, S.; Inoue, N.; Kunugi, T.; Shibahara, M. Large-scale molecular dynamics simulation of sputtering process with glancing-angle Ar cluster impact on 4H-SiC. *Nucl. Instrum. Meth. B* **2009**, *267*, 3258–3262. [CrossRef]
65. Triendl, F.; Pfusterschmied, G.; Schwarz, S.; Pobegen, G.; Konrath, J.P.; Schmid, U. Barrier height tuning by inverse sputter etching at poly-Si/4H-SiC heterojunction diodes. *Semicond. Sci. Technol.* **2021**, *36*, 055021. [CrossRef]
66. Prskalo, A.P.; Schmauder, S.; Ziebert, C.; Ye, J.; Ulrich, S. Molecular dynamics simulations of the sputtering of SiC and Si3N4. *Surf. Coat. Technol.* **2010**, *204*, 2081–2084. [CrossRef]
67. Sun, W.; Liu, H.; Lin, L.; Zhao, C.; Lu, X.; He, P.; Gou, F. Molecular Dynamics Simulations of Atomic H Etching SiC Surface. *Phys. Procedia* **2012**, *32*, 539–544. [CrossRef]
68. Gou, F.; Zen, L.T.; Meng, C.L. Molecular dynamics simulations of CF3 etching of SiC. *Thin Solid Films* **2008**, *516*, 1832–1837. [CrossRef]
69. Lu, X.; Ning, J.; Qin, Y.; Qiu, Q.; Chuanwu, Z.; Ying, Y.; Ming, J.; Gou, F. Substrate temperature effect on F+ etching of SiC: Molecular dynamics simulation. *Nucl. Instrum. Meth. B* **2009**, *267*, 3235–3237. [CrossRef]
70. Xue, L.H.; Feng, G.; Wu, G.; Wang, S.Z.; Li, R.; Han, X.; Sun, Y.M.; Liu, S. Study of the deposition of nanopillar-patterned 4H-SiC by molecular dynamics simulation. *Appl. Surf. Sci.* **2022**, *579*, 152209. [CrossRef]
71. Teng, M.; He, X.D.; Sun, Y. Composition and nanohardness of SiC films deposited by electron beam physical vapor deposition. *Int. J. Mod. Phys. B* **2009**, *23*, 1910–1915. [CrossRef]
72. Kim, J.Y.; Lee, B.W.; Nam, H.S.; Kwon, D. Effect of substrate temperature on structure and intrinsic stress in vapor-deposited amorphous silicon carbide film. *Thin Solid Films* **2004**, *467*, 294–299. [CrossRef]
73. Kim, J.Y.; Lee, B.W.; Nam, H.S.; Kwon, D. Molecular dynamics analysis of structure and intrinsic stress in amorphous silicon carbide film with deposition process parameters. *Mater. Sci. Forum* **2004**, *449–452*, 97–100. [CrossRef]
74. Gao, Y.; Yan, W.J.; Gao, T.H.; Chen, Q.; Yang, W.S.; Xie, Q.; Tian, Z.A.; Liang, Y.C.; Luo, J.; Li, L.X. Properties of the structural defects during SiC-crystal-induced crystallization on the solid-liquid interface. *Mater. Sci. Semicond. Process.* **2020**, *116*, 105155. [CrossRef]
75. Narumi, T.; Shibuta, Y.; Yoshikawa, T. Molecular dynamics simulation of interfacial growth of SiC from Si-C solution on different growth planes. *J. Cryst. Growth* **2018**, *494*, 36–43. [CrossRef]

76. Nguyen, H.T.T. Structural evolution of SiC sheet in a graphene-based in-plane hybrid system upon heating using molecular dynamics simulation. *Thin Solid Films* **2021**, *739*, 138992. [CrossRef]
77. Tranh, D.T.N.; Hoang, V.V.; Hanh, T.T.T. Modeling glassy SiC nanoribbon by rapidly cooling from the liquid: An affirmation of appropriate potentials. *Phys. B* **2021**, *608*, 412746. [CrossRef]
78. Hoang, V.V. Melting and pre-melting of two-dimensional crystalline SiC nanoribbons. *Phys. E* **2022**, *137*, 115012. [CrossRef]
79. Hoang, V.V.; Giang, N.H.; Dong, T.Q.; Bubanja, V. Atomic structure and rippling of amorphous two-dimensional SiC nanoribbons—MD simulations. *Comput. Mater. Sci.* **2022**, *203*, 111123. [CrossRef]
80. Liu, Y.T.; Liu, R.Z.; Liu, M.L.; Chang, J.X. Synthesis of SiC@Al2O3 core-shell nanoparticles for dense SiC sintering. *Particuology* **2019**, *44*, 80–89. [CrossRef]
81. Xin, Z.H.; Zhang, C.Y.; Yu, M.; Jayanthi, C.S.; Wu, S.Y. Shedding light on the self-assembly of stable SiC based cage nanostructures: A comprehensive molecular dynamics study. *Comput. Mater. Sci.* **2014**, *84*, 49–62. [CrossRef]
82. Wu, J.T.; Xu, Z.W.; Zhao, J.L.; Rommel, M.; Nordlund, K.; Ren, F.; Fang, F.Z. MD simulation of two-temperature model in ion irradiation of 3C-SiC: Effects of electronic and nuclear stopping coupling, ion energy and crystal orientation. *J. Nucl. Mater.* **2021**, *557*, 153313. [CrossRef]
83. Nguyen, B.N.; Gao, F.; Henager, C.H.; Kurtz, R.J. Prediction of thermal conductivity for irradiated SiC/SiC composites by informing continuum models with molecular dynamics data. *J. Nucl. Mater.* **2014**, *448*, 364–372. [CrossRef]
84. Zarkadoula, E.; Samolyuk, G.; Zhang, Y.W.; Weber, W.J. Electronic stopping in molecular dynamics simulations of cascades in 3C-SiC. *J. Nucl. Mater.* **2020**, *540*, 152371. [CrossRef]
85. Samolyuk, G.D.; Osetsky, Y.N.; Stoller, R.E. Molecular dynamics modeling of atomic displacement cascades in 3C-SiC: Comparison of interatomic potentials. *J. Nucl. Mater.* **2015**, *465*, 83–88. [CrossRef]
86. He, B.; Xue, J.M.; Zou, X.Q.; Wang, Y.G. Molecular Dynamics Study on the Irradiation-Induced Damage in SiC. *Acta Sci. Nat. Univ. Pekin.* **2009**, *45*, 385–389. [CrossRef]
87. Li, B.S.; Zhang, C.; Liu, H.P.; Xu, L.J.; Wang, X.; Yang, Z.; Ge, F.F.; Gao, W.; Shen, T.L. Microstructural and elemental evolution of polycrystalline α-SiC irradiated with ultra-high-fluence helium ions before and after annealing. *Fusion. Eng. Des.* **2020**, *154*, 111511. [CrossRef]
88. Ran, Q.; Zhou, Y.; Zou, Y.; Wang, J.; Duan, Z.A.; Sun, Z.P.; Fu, B.Q.; Gao, S.X. Molecular dynamics simulation of displacement cascades in cubic silicon carbide. *Nucl. Mater. Energy* **2021**, *27*, 100957. [CrossRef]
89. Backman, M.; Toulemonde, M.; Pakarinen, O.H.; Juslin, N.; Djurabekova, F.; Nordlund, K.; Debelle, A.; Weber, W.J. Molecular dynamics simulations of swift heavy ion induced defect recovery in SiC. *Comput. Mater. Sci.* **2013**, *67*, 261–265. [CrossRef]
90. Peterson, R.; Senesky, D. Modeling of radiation-induced defect recovery in 3C-SiC under high field bias conditions. *Comput. Mater. Sci.* **2019**, *161*, 10–15. [CrossRef]
91. Li, Y.Y.; Xiao, W.; Li, H.L. Molecular dynamics simulation of C/Si ratio effect on the irradiation swelling of β-SiC. *J. Nucl. Mater.* **2016**, *480*, 75–79. [CrossRef]
92. Tian, J.T.; Feng, Q.J.; Zheng, J.; Zhou, W.; Li, X.; Liang, X.B.; Liu, D.F. Molecular Dynamics Simulations of Radiation-induced Swelling and Amorphization in a Single Crystal of 3C-SiC. *Mater. Rep.* **2022**, *36*, 20100248-5. [CrossRef]
93. Zhu, S.; Mizuno, M.; Kagawa, Y.; Mutoh, Y. Monotonic tension, fatigue and creep behavior of SiC-fiber-reinforced SiC-matrix composites: A review. *Compos. Sci. Technol.* **1999**, *59*, 833–851. [CrossRef]
94. Feng, L.X.; Li, W.H.; Hahn, E.N.; Branicio, P.S.; Zhang, X.Q.; Yao, X.H. Structural phase transition and amorphization in hexagonal SiC subjected to dynamic loading. *Mech. Mater.* **2022**, *164*, 104139. [CrossRef]
95. Lee, W.H.; Yao, X.H.; Jian, W.R.; Han, Q. High-velocity shock compression of SiC via molecular dynamics simulation. *Comput. Mater. Sci.* **2015**, *98*, 297–303. [CrossRef]
96. Zhang, J.Y.; Branicio, P.S. Molecular Dynamics Simulations of Plane Shock Loading in SiC. *Procedia Eng.* **2014**, *75*, 150–153. [CrossRef]

Disclaimer/Publisher's Note: The statements, opinions and data contained in all publications are solely those of the individual author(s) and contributor(s) and not of MDPI and/or the editor(s). MDPI and/or the editor(s) disclaim responsibility for any injury to people or property resulting from any ideas, methods, instructions or products referred to in the content.